Evidence for the decay $B^0 \to K^+ K^- \pi^0$

V. Gaur,[55] G. B. Mohanty,[55] T. Aziz,[55] I. Adachi,[12] H. Aihara,[60] D. M. Asner,[46] V. Aulchenko,[2] T. Aushev,[21]
A. M. Bakich,[54] A. Bala,[47] K. Belous,[18] V. Bhardwaj,[38] B. Bhuyan,[14] G. Bonvicini,[66] A. Bozek,[42] M. Bračko,[31,22]
T. E. Browder,[11] P. Chang,[41] V. Chekelian,[32] A. Chen,[39] P. Chen,[41] B. G. Cheon,[10] R. Chistov,[21] K. Cho,[25] V. Chobanova,[32]
S. -K. Choi,[9] Y. Choi,[53] D. Cinabro,[66] J. Dalseno,[32,56] M. Danilov,[21,34] Z. Doležal,[3] Z. Drásal,[3] A. Drutskoy,[21,34]
D. Dutta,[14] K. Dutta,[14] S. Eidelman,[2] H. Farhat,[66] M. Feindt,[24] T. Ferber,[5] A. Frey,[8] N. Gabyshev,[2] S. Ganguly,[66]
R. Gillard,[66] Y. M. Goh,[10] B. Golob,[29,22] J. Haba,[12] H. Hayashii,[38] Y. Horii,[37] Y. Hoshi,[58] W. -S. Hou,[41] H. J. Hyun,[27]
T. Iijima,[37,36] A. Ishikawa,[59] R. Itoh,[12] Y. Iwasaki,[12] T. Julius,[33] D. H. Kah,[27] J. H. Kang,[68] T. Kawasaki,[44] C. Kiesling,[32]
H. J. Kim,[27] J. B. Kim,[26] J. H. Kim,[25] K. T. Kim,[26] M. J. Kim,[27] Y. J. Kim,[25] K. Kinoshita,[4] J. Klucar,[22] B. R. Ko,[26]
P. Kodyš,[3] S. Korpar,[31,22] P. Križan,[29,22] R. Kumar,[49] T. Kumita,[62] Y. -J. Kwon,[68] J. S. Lange,[6] S. -H. Lee,[26] J. Li,[52] Y. Li,[65]
J. Libby,[15] C. Liu,[51] D. Liventsev,[12] P. Lukin,[2] D. Matvienko,[2] K. Miyabayashi,[38] H. Miyata,[44] N. Muramatsu,[50]
R. Mussa,[20] E. Nakano,[45] M. Nakao,[12] M. Nayak,[15] E. Nedelkovska,[32] N. K. Nisar,[55] S. Nishida,[12] O. Nitoh,[63] S. Ogawa,[57]
S. Okuno,[23] Y. Onuki,[60] W. Ostrowicz,[42] P. Pakhlov,[21,34] G. Pakhlova,[21] H. Park,[27] H. K. Park,[27] T. K. Pedlar,[30]
R. Pestotnik,[22] M. Petrič,[22] L. E. Piilonen,[65] M. Ritter,[32] M. Röhrken,[24] A. Rostomyan,[5] H. Sahoo,[11] T. Saito,[59] Y. Sakai,[12]
S. Sandilya,[55] D. Santel,[4] T. Sanuki,[59] Y. Sato,[59] V. Savinov,[48] O. Schneider,[28] G. Schnell,[1,13] C. Schwanda,[17]
D. Semmler,[6] K. Senyo,[67] O. Seon,[36] M. E. Sevior,[33] M. Shapkin,[18] C. P. Shen,[36] T. -A. Shibata,[61] J. -G. Shiu,[41]
A. Sibidanov,[54] F. Simon,[32,56] J. B. Singh,[47] R. Sinha,[19] P. Smerkol,[22] Y. -S. Sohn,[68] A. Sokolov,[18] E. Solovieva,[21]
M. Starič,[22] M. Steder,[5] M. Sumihama,[7] T. Sumiyoshi,[62] U. Tamponi,[20,64] G. Tatishvili,[46] Y. Teramoto,[45] T. Tsuboyama,[12]
M. Uchida,[61] S. Uehara,[12] T. Uglov,[21,35] Y. Unno,[10] S. Uno,[12] S. E. Vahsen,[11] C. Van Hulse,[1] P. Vanhoefer,[32] G. Varner,[11]
K. E. Varvell,[54] V. Vorobyev,[2] M. N. Wagner,[6] C. H. Wang,[40] P. Wang,[16] X. L. Wang,[65] M. Watanabe,[44] Y. Watanabe,[23]
K. M. Williams,[65] E. Won,[26] B. D. Yabsley,[54] Y. Yamashita,[43] S. Yashchenko,[5] Y. Yusa,[44] V. Zhilich,[2] and A. Zupanc[24]

(Belle Collaboration)

[1]*University of the Basque Country, UPV/EHU, 48080 Bilbao*
[2]*Budker Institute of Nuclear Physics SB RAS and Novosibirsk State University, Novosibirsk 630090*
[3]*Faculty of Mathematics and Physics, Charles University, 121 16 Prague*
[4]*University of Cincinnati, Cincinnati, Ohio 45221*
[5]*Deutsches Elektronen-Synchrotron, 22607 Hamburg*
[6]*Justus-Liebig-Universität Gießen, 35392 Gießen*
[7]*Gifu University, Gifu 501-1193*
[8]*II. Physikalisches Institut, Georg-August-Universität Göttingen, 37073 Göttingen*
[9]*Gyeongsang National University, Chinju 660-701*
[10]*Hanyang University, Seoul 133-791*
[11]*University of Hawaii, Honolulu, Hawaii 96822*
[12]*High Energy Accelerator Research Organization (KEK), Tsukuba 305-0801*
[13]*Ikerbasque, 48011 Bilbao*
[14]*Indian Institute of Technology Guwahati, Assam 781039*
[15]*Indian Institute of Technology Madras, Chennai 600036*
[16]*Institute of High Energy Physics, Chinese Academy of Sciences, Beijing 100049*
[17]*Institute of High Energy Physics, Vienna 1050*
[18]*Institute for High Energy Physics, Protvino 142281*
[19]*Institute of Mathematical Sciences, Chennai 600113*
[20]*INFN - Sezione di Torino, 10125 Torino*
[21]*Institute for Theoretical and Experimental Physics, Moscow 117218*
[22]*J. Stefan Institute, 1000 Ljubljana*
[23]*Kanagawa University, Yokohama 221-8686*
[24]*Institut für Experimentelle Kernphysik, Karlsruher Institut für Technologie, 76131 Karlsruhe*
[25]*Korea Institute of Science and Technology Information, Daejeon 305-806*
[26]*Korea University, Seoul 136-713*
[27]*Kyungpook National University, Daegu 702-701*
[28]*École Polytechnique Fédérale de Lausanne (EPFL), Lausanne 1015*
[29]*Faculty of Mathematics and Physics, University of Ljubljana, 1000 Ljubljana*
[30]*Luther College, Decorah, Iowa 52101*
[31]*University of Maribor, 2000 Maribor*

091101-1

^{32}*Max-Planck-Institut für Physik, 80805 München*
^{33}*School of Physics, University of Melbourne, Victoria 3010*
^{34}*Moscow Physical Engineering Institute, Moscow 115409*
^{35}*Moscow Institute of Physics and Technology, Moscow Region 141700*
^{36}*Graduate School of Science, Nagoya University, Nagoya 464-8602*
^{37}*Kobayashi-Maskawa Institute, Nagoya University, Nagoya 464-8602*
^{38}*Nara Women's University, Nara 630-8506*
^{39}*National Central University, Chung-li 32054*
^{40}*National United University, Miao Li 36003*
^{41}*Department of Physics, National Taiwan University, Taipei 10617*
^{42}*H. Niewodniczanski Institute of Nuclear Physics, Krakow 31-342*
^{43}*Nippon Dental University, Niigata 951-8580*
^{44}*Niigata University, Niigata 950-2181*
^{45}*Osaka City University, Osaka 558-8585*
^{46}*Pacific Northwest National Laboratory, Richland, Washington 99352*
^{47}*Panjab University, Chandigarh 160014*
^{48}*University of Pittsburgh, Pittsburgh, Pennsylvania 15260*
^{49}*Punjab Agricultural University, Ludhiana 141004*
^{50}*Research Center for Electron Photon Science, Tohoku University, Sendai 980-8578*
^{51}*University of Science and Technology of China, Hefei 230026*
^{52}*Seoul National University, Seoul 151-742*
^{53}*Sungkyunkwan University, Suwon 440-746*
^{54}*School of Physics, University of Sydney, New South Wales 2006*
^{55}*Tata Institute of Fundamental Research, Mumbai 400005*
^{56}*Excellence Cluster Universe, Technische Universität München, 85748 Garching*
^{57}*Toho University, Funabashi 274-8510*
^{58}*Tohoku Gakuin University, Tagajo 985-8537*
^{59}*Tohoku University, Sendai 980-8578*
^{60}*Department of Physics, University of Tokyo, Tokyo 113-0033*
^{61}*Tokyo Institute of Technology, Tokyo 152-8550*
^{62}*Tokyo Metropolitan University, Tokyo 192-0397*
^{63}*Tokyo University of Agriculture and Technology, Tokyo 184-8588*
^{64}*University of Torino, 10124 Torino*
^{65}*Center for Neutrino Physics, Virginia Polytechnic Institute and State University, Blacksburg, Virginia 24061*
^{66}*Wayne State University, Detroit, Michigan 48202*
^{67}*Yamagata University, Yamagata 990-8560*
^{68}*Yonsei University, Seoul 120-749*

We report a search for charmless hadronic decays of neutral B mesons to the final state $K^+K^-\pi^0$. The results are based on a 711 fb^{-1} data sample that contains 772×10^6 $B\bar{B}$ pairs, and was collected at the $\Upsilon(4S)$ resonance with the Belle detector at the KEKB asymmetric-energy e^+e^- collider. We find the first evidence for this decay with a significance of 3.5 standard deviations and measure its branching fraction as $\mathcal{B}(B^0 \rightarrow K^+K^-\pi^0) = [2.17 \pm 0.60(\text{stat}) \pm 0.24(\text{syst})] \times 10^{-6}$.

The B-meson decay $B^0 \rightarrow K^+K^-\pi^0$ is suppressed in the standard model (SM) and thus offers a useful probe for new physics beyond the SM. Figure 1 shows typical Feynman diagrams that contribute to this decay. The dominant one is the color- and Cabibbo-suppressed $b \rightarrow u$ tree transition followed by the internal W exchange diagram leading to $B^0 \rightarrow K^{*\pm}K^{\mp}$ with $K^{*\pm} \rightarrow K^{\pm}\pi^0$. The latter diagram dominates in the decay $B^0 \rightarrow K^+K^-$, for which only upper limits have been placed on the branching fraction [1–4]. This is in contrast to the related decays (having two kaons in the final state) that are already observed such as $B^0 \rightarrow K^0\bar{K}^0$, $B^+ \rightarrow K^0K^+$ [4,5], and $B^+ \rightarrow K^+K^-\pi^+$

[6,7], where the $b \rightarrow d$ gluonic penguin amplitude can contribute as well [8].

The three-body decay $B^0 \rightarrow K^+K^-\pi^0$ has not yet been observed, with only one measured upper limit of $\mathcal{B}(B^0 \rightarrow K^+K^-\pi^0) < 19 \times 10^{-6}$ at 90% confidence level from the CLEO Collaboration [9]. Intermediate resonant modes that decay preferentially to this final state have also not been seen. A search for a related channel by Belle has set an upper limit of $\mathcal{B}(B^0 \rightarrow \phi\pi^0) < 1.5 \times 10^{-7}$ [10]. The latter mode is quite sensitive to possible beyond-the-SM contributions; a branching fraction of $\mathcal{O}(10^{-7})$ would constitute evidence for new physics [11]. No experimental
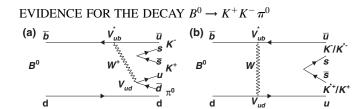
FIG. 1. Typical Feynman diagrams that contribute to the decay $B^0 \to K^+ K^- \pi^0$: (a) $b \to u$ tree and (b) internal W exchange.

information is available for other potential resonance modes such as $K^*(892)^{\pm} K^{\mp}$, $K_0^*(1430)^{\pm} K^{\mp}$, and $f_0(980)\pi^0$. For the decay $B^0 \to K^*(892)^{\pm} K^{\mp}$ dominated by internal W exchange [Fig. 1(b)], the branching fraction is predicted to be in the range 10^{-8} to 10^{-7} [12–14].

Another motivation for the study of $B^0 \to K^+ K^- \pi^0$ comes from the observation of $B^+ \to K^+ K^- \pi^+$ by the *BABAR* Collaboration [6]. In particular, an unexpected structure is seen near 1.5 GeV/c^2 in the $K^+ K^-$ invariant-mass spectrum, which accounts for about half of the total events. Similar structures have also been observed in the Dalitz plots of $B^+ \to K^+ K^- K^+$ and $B^0 \to K^+ K^- K^0$ decays [15–17]. If these structures are due to a particular $K^+ K^-$ resonant state, it should show up in $B^0 \to K^+ K^- \pi^0$; on the other hand, if it is a reflection from the $b \to d$ penguin, it will not contribute to $K^+ K^- \pi^0$. Since the u and d quarks are spectators in the $b \to u$ tree diagram [Fig. 1(a)] for $B^+ \to K^+ K^- \pi^+$ and $B^0 \to K^+ K^- \pi^0$, respectively, one can estimate the branching fraction for the latter using the *BABAR* results. Assuming isospin symmetry and the $b \to u$ transition to be the main contributor to $B^0 \to K^+ K^- \pi^0$, we expect its branching fraction to be at the level of 3×10^{-6}, which is well within Belle's reach.

Our results are based on a data sample containing 772×10^6 $B\bar{B}$ pairs collected at the $\Upsilon(4S)$ resonance with the Belle detector [18] at the KEKB asymmetric-energy $e^+ e^-$ (3.5 on 8.0 GeV) collider [19]. The principal detector components used in the study are a silicon vertex detector, a 50-layer central drift chamber (CDC), an array of aerogel threshold Cherenkov counters (ACC), a barrel-like arrangement of time-of-flight scintillation counters (TOF), and a CsI(Tl) crystal electromagnetic calorimeter (ECL). All these components are located inside a 1.5 T solenoidal magnetic field.

To reconstruct $B^0 \to K^+ K^- \pi^0$ decay candidates, we combine two oppositely charged kaons with a π^0 meson. Each track candidate must have a minimum transverse momentum of 100 MeV/c, and a distance of closest approach with respect to the interaction point of less than 0.2 cm in the transverse r-ϕ plane and less than 5.0 cm along the z axis, where the z axis is defined by the direction opposite the e^+ beam. Identification of charged kaons is based on a likelihood ratio $R_{K/\pi} = \frac{\mathcal{L}_K}{\mathcal{L}_K + \mathcal{L}_\pi}$, where $\mathcal{L}_K$ and $\mathcal{L}_\pi$ denote the individual likelihoods for kaons and pions, respectively, calculated using specific ionization in the CDC, time-of-flight information from the TOF, and the

number of photoelectrons from the ACC. A requirement $R_{K/\pi} > 0.6$ is applied to select both kaon candidates. The kaon identification efficiency is approximately 86% and the probability of misidentifying a pion as a kaon is 11%. We reconstruct π^0 candidates from photon pairs that have an invariant mass between 112 and 156 MeV/c^2, corresponding to $\pm 3.5\sigma$ around the nominal π^0 mass [20]. These photons are reconstructed from neutral clusters in the ECL with energy above 60 (100) MeV in the barrel (endcap) region. In addition, requirements on the π^0 decay helicity angle, $|\cos \theta_{\rm hel}| < 0.95$, and the π^0 mass-constrained fit statistic, $\chi^2_{\rm mass} < 50$, are imposed. Here, $\theta_{\rm hel}$ is the angle between one of the daughter photons and the B momentum in the π^0 rest frame.

B-meson candidates are identified using two kinematic variables: beam-energy constrained mass, $M_{\rm bc} = \sqrt{E_{\rm beam}^2 - |\sum_i \vec{p}_i|^2}$, and energy difference, $\Delta E = \sum_i E_i - E_{\rm beam}$, where $E_{\rm beam}$ is the beam energy, and $\vec{p}_i$ and E_i are the momentum and energy, respectively, of the ith daughter of the reconstructed B in the center-of-mass (CM) frame. We retain events with 5.271 GeV/$c^2 < M_{\rm bc} <$ 5.289 GeV/c^2 and -0.30 GeV $< \Delta E < 0.15$ GeV for further analysis. The $M_{\rm bc}$ requirement corresponds to approximately $\pm 3\sigma$ around the nominal B^0 mass [20]; we apply a looser window of $(-12\sigma, +6\sigma)$ around $\Delta E = 0$ because it is used in the fitter (as described below). The average number of B candidates found per event is 1.3. In events with multiple B candidates, we choose the one(s) whose π^0 has the lowest $\chi^2_{\rm mass}$ value. If more than one B candidate shares the same π^0 meson, the candidate yielding the best B^0 vertex fit is selected.

The dominant background is from the $e^+ e^- \to q\bar{q}$ ($q = u, d, s, c$) continuum process. To suppress this background, observables based on the event topology are utilized. The event shape in the CM frame is more spherical for $B\bar{B}$ events and jetlike for continuum events. We employ a neural network [21] to combine the following six input variables: the Fisher discriminant formed from 16 modified Fox-Wolfram moments [22], the cosine of the angle between the B momentum and the z axis, the cosine of the angle between the B thrust and the z axis, the cosine of the angle between the thrust axis of the B candidate and that of the rest of the event, the ratio of the second- to the zeroth-order Fox-Wolfram moments (all of these quantities being calculated in the CM frame), and the separation along the z axis between the vertex of the B candidate and that of the remaining tracks. The training and optimization of the neural network are accomplished with signal and $q\bar{q}$ Monte Carlo (MC) simulated events. The signal MC sample is generated with the EVTGEN program [23] by assuming a three-body phase space. We require the neural network output (C_{NB}) to be above 0.2 to substantially reduce the continuum background. The relative signal efficiency due to this requirement is approximately 88%, whereas the continuum suppression achieved is close to

92%. The remainder of the C_{NB} distribution peaks strongly near 1.0 for signal, and thus we have difficulty in modeling it with an analytic function. However, its transformed variable

$$C'_{NB} = \log\left[\frac{C_{NB} - C_{NB,\min}}{C_{NB,\max} - C_{NB}}\right], \qquad (1)$$

where $C_{NB,\min} = 0.2$ and $C_{NB,\max} = 1.0$, has a distribution with a Gaussian-like tail.

The background due to B decays via the dominant $b \to c$ transition is studied with an MC sample of a collection of such decays. The resulting M_{bc} distribution is found to peak strongly in the signal region. We also observe two peaks in the K^+K^- invariant-mass spectrum that corresponds to the contributions from (a) $D^0 \to K^+K^-$ peaking at the nominal D^0 mass [20], and (b) $D^0 \to K^-\pi^+$ with the peak shifted slightly from the D^0 mass owing to K-π misidentification. To suppress these peaking contributions, we exclude candidates for which the invariant mass of the K^+K^- system lies in the range of $[1846, 1884]$ MeV$/c^2$ (about $\pm 5\sigma$ around the nominal D^0 mass). In the case of (b), we use the pion hypothesis for one of the tracks. The surviving events constitute the "generic $B\bar{B}$" background.

There are a few background modes that contribute in the M_{bc} signal region having the ΔE peak shifted to positive values. The so-called "rare peaking" background modes arising mostly from K-π misidentification are identified with a $B\bar{B}$ MC sample in which one of the B mesons decays via $b \to u$, d, s transitions with known or estimated branching fractions. The rare peaking background includes the $B^0 \to K^+\pi^-\pi^0$ nonresonant decay as well as possible intermediate resonant modes that result in the $K^+\pi^-\pi^0$ final state, such as $B^0 \to K^*(892)^0\pi^0$ and $B^0 \to K^*(892)^+\pi^-$. The events that remain after removing the signal and rare peaking components comprise the "rare combinatorial" background.

The signal yield is obtained with an unbinned extended maximum likelihood fit to the two-dimensional distributions of ΔE and C'_{NB}. We define a probability density function (PDF) for each event category j (signal, $q\bar{q}$, generic $B\bar{B}$, rare peaking, and rare combinatorial $B\bar{B}$ backgrounds):

$$\mathcal{P}^i_j \equiv \mathcal{P}_j(\Delta E^i)\mathcal{P}_j(C'^i_{NB}), \qquad (2)$$

where i denotes the event index. Since the correlation between ΔE and C'_{NB} is found to be negligible, the product of two individual PDFs is a good approximation for the combined PDF. We apply a tight requirement on M_{bc} rather than including it in the fitter because it exhibits an irreducible correlation with ΔE owing to shower leakage in the ECL. The extended likelihood function is

$$\mathcal{L} = \exp\left(-\sum_j n_j\right) \times \prod_i\left[\sum_j n_j\mathcal{P}^i_j\right], \qquad (3)$$

TABLE I. List of PDFs used to model the ΔE and C'_{NB} distributions for various event categories. G, AG, CB, and Poly2 denote Gaussian, asymmetric Gaussian, Crystal Ball [24], and second-order Chebyshev polynomial function, respectively.

Event category	ΔE	C'_{NB}
CR signal	CB + AG	3 AG
SCF signal	histogram	histogram
Continuum $q\bar{q}$	Poly2	AG
Generic $B\bar{B}$	Poly2	AG
Rare peaking $B\bar{B}$	2 G	AG
Rare combinatorial $B\bar{B}$	histogram	3 AG

where n_j is the yield of event category j. The correctly reconstructed (CR) and misreconstructed fragments of the B-meson decay referred to as self-crossfeed (SCF) components of the signal are considered distinct in the fitter: their combined PDF is $n_{\text{sig}} \times [(1 - f)\mathcal{P}_{\text{CR}} + f\mathcal{P}_{\text{SCF}}]$, where n_{sig} is the total signal yield and f is the SCF fraction fixed to the MC expected value of 3%.

Table I lists the PDF shapes used to model the ΔE and C'_{NB} distributions for each event category. Distributions that are difficult to parametrize analytically are modeled with histograms. The yields for all event categories except the rare peaking $B\bar{B}$ background are allowed to vary in the fit. We fix the yield of the rare peaking $B\bar{B}$ component to the value calculated using the branching fraction measured in an amplitude analysis of $B^0 \to K^+\pi^-\pi^0$ [25]. The following PDF shape parameters of the $q\bar{q}$ background are floated: the two parameters of the second-order Chebyshev polynomial used for ΔE, and the mean and two widths of the asymmetric Gaussian function used to model C'_{NB}. The PDF shapes for signal and other background components are fixed to the corresponding MC expectations. We adjust the parameters of the signal ΔE and C'_{NB} PDFs to account for possible data-MC differences, according to the values obtained with a large-statistics control sample of $B^+ \to \bar{D}^0(K^+\pi^-\pi^0)\pi^+$. The same correction factors are also applied for the rare peaking $B\bar{B}$ background.

Figure 2 shows the ΔE and C'_{NB} projections of the fit applied to 39066 candidate events. We obtain 299 ± 83 signal events (n_{sig}), 32167 ± 428 continuum $q\bar{q}$, 3814 ± 517 generic $B\bar{B}$, and 2691 ± 321 rare combinatorial $B\bar{B}$ background events. The statistical significance of the signal is 3.8 standard deviations. It is calculated as $\sqrt{2\log(\mathcal{L}_0/\mathcal{L}_{\max})}$, where $\mathcal{L}_0$ and $\mathcal{L}_{\max}$ are the fit likelihood values with the signal yield set to zero and the best-fit case, respectively. The obtained background yields are consistent with the respective MC predictions. The signal decay branching fraction is calculated as

$$\mathcal{B}(B^0 \to K^+K^-\pi^0) = \frac{n_{\text{sig}}}{N_{B\bar{B}} \times \varepsilon_{\text{rec}} \times r_{K/\pi}}, \qquad (4)$$

RAPID COMMUNICATIONS

EVIDENCE FOR THE DECAY $B^0 \to K^+K^-\pi^0$ .... PHYSICAL REVIEW D **87**, 091101(R) (2013)
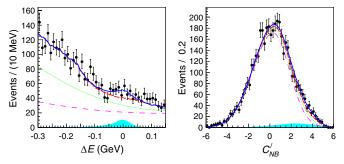
FIG. 2 (color online). Projections of candidate events onto (left) ΔE for $C'_{NB} > 3$ and (right) C'_{NB} for $|\Delta E| < 30$ MeV. Points with error bars are the data, solid (blue) curves are the total PDF, dashed (red) curves are the total background, dotted (green) curves are the sum of continuum $q\bar{q}$ and generic $B\bar{B}$ backgrounds, dash-dotted (magenta) curves are the continuum $q\bar{q}$ background, and filled (cyan) regions show the signal.

where $N_{B\bar{B}}$ is the total number of $B\bar{B}$ pairs (772×10^6), $\varepsilon_{\mathrm{rec}}$ is the signal reconstruction efficiency (19.6%) obtained in the study described below, and $r_{K/\pi}$ denotes the kaon-identification efficiency correction factor that accounts for a small data-MC difference. It is given by

$$r_{K/\pi} \equiv \varepsilon_{K/\pi}^{\mathrm{data}} / \varepsilon_{K/\pi}^{\mathrm{MC}}, \qquad (5)$$

where $\varepsilon_{K/\pi}^{\mathrm{data}}$ ($\varepsilon_{K/\pi}^{\mathrm{MC}}$) is the efficiency of the $R_{K/\pi}$ requirement in data (MC simulations). The $r_{K/\pi}$ value per kaon track is 0.95, resulting in a total $r_{K/\pi} = 0.95^2 = 0.90$ for two kaons. We have verified that the $R_{K/\pi}$ correction factor is almost constant over the Dalitz plot. For the branching fraction calculation presented in Eq. (4), we assume equal production of $B^0\bar{B}^0$ and B^+B^- pairs at the $\Upsilon(4S)$ resonance. The resulting value is

$$\mathcal{B}(B^0 \to K^+K^-\pi^0) = [2.17 \pm 0.60 \pm 0.24] \times 10^{-6},$$
$$(6)$$

where the uncertainties are statistical and systematic, respectively. The contributions to the systematic uncertainty are discussed below and listed in Table II.

The uncertainties due to the PDF shape parameters are estimated by varying all fixed parameters by $\pm 1\sigma$. To assign a systematic error for the histogram PDF used to model ΔE for the rare combinatorial component, we carry out a series of fits by fluctuating each of the histogram bin contents according to the Poisson distribution. The spread of the fitted signal yields is taken as the systematic error. We also vary the yield of final states that dominantly contribute to that component according to their errors. As we use a fairly complex function (a sum of three asymmetric Gaussians) to model the signal C'_{NB} PDF shape, we evaluate possible systematics due to the uncertainty in the functional dependence by checking other alternatives. This systematic contribution is denoted as "Signal C'_{NB} functional dependence" in Table II. The uncertainty due to the

TABLE II. Summary of various systematic uncertainties. The first and second horizontal blocks denote the additive and multiplicative systematic uncertainties, respectively.

Source	Uncertainties (%)	
Signal PDF	+3.4	−2.9
Generic $B\bar{B}$ PDF	+2.4	−3.1
Combinatorial background PDF	+1.3	−2.0
Peaking background PDFs	+1.7	−1.9
Fixed histogram PDF	+1.7	−2.0
Signal C'_{NB} functional dependence	+2.3	−2.3
Fixed SCF fraction	+1.7	−1.7
Fit bias	+2.4	−2.4
Continuum suppression	+2.2	−2.2
Requirement on M_{bc}	+1.5	−0.2
Kaon ID requirement	+1.9	−1.9
π^0 detection efficiency	+4.0	−4.0
Charged-track reconstruction	+0.7	−0.7
Efficiency variation over Dalitz plot	+7.5	−7.5
Number of $B\bar{B}$ pairs	+1.4	−1.4
Total	+11.1	−11.3

fixed (small) SCF fraction is estimated without knowing *a priori* how these SCF events vary across the Dalitz plot. We adopt a conservative approach to vary the SCF fraction by $\pm 50\%$ when calculating the associated systematic error. The potential fit bias is evaluated by performing an ensemble test comprising 200 pseudoexperiments, where the signal and rare peaking background components are embedded from the corresponding MC samples, and the PDF shapes are used to generate the data for the other event categories. We obtain an almost Gaussian pull distribution of unit width, and add the mean and error on the pull in quadrature for assigning the systematics. Uncertainty due to continuum suppression is derived with the control sample by comparing the nominal fit result with that obtained without any C_{NB} requirement. We estimate the error due to the M_{bc} requirement by varying its nominal selection threshold by the resolution. The $D^{*+} \to D^0(K^-\pi^+)\pi^+$ control sample is used to determine the systematic uncertainty due to the $R_{K/\pi}$ requirement. The systematic uncertainty due to π^0 reconstruction is evaluated by comparing data-MC differences of the yield ratio between $\eta \to \pi^0\pi^0\pi^0$ and $\eta \to \pi^+\pi^-\pi^0$. We use partially reconstructed $D^{*+} \to D^0(K_S^0\pi^+\pi^-)\pi^+$ decays to assign the systematic uncertainty due to charged-track reconstruction (0.35% per track). To account for the possible variation of efficiency across the Dalitz-plot distribution, we calculate a weighted signal reconstruction efficiency by fitting different regions of that distribution. The mean value is used to obtain the branching fraction and the error is taken as the systematic contribution due to the efficiency variation. The total systematic uncertainty is calculated by summing all these uncertainties in quadrature. To determine the significance of our measurement, we use a convolution of the statistical likelihood with a Gaussian function of width
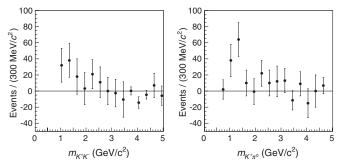
FIG. 3. Signal yield distributions as a function of (left) $m(K^+K^-)$ with $m(K^+\pi^0) > 1.5$ GeV/c^2 and (right) $m(K^+\pi^0)$ with $m(K^+K^-) > 2.0$ GeV/c^2. Each point is obtained from a two-dimensional [ΔE, C'_{NB}] fit.

equal to the additive systematic errors that only affect the signal yield. The total significance, including these uncertainties, is 3.5 standard deviations.

To elucidate the nature of the observed signal, especially whether there are contributions from the decays with intermediate resonant states, we study the K^+K^- and $K^+\pi^0$ invariant mass distributions. We perform the [ΔE, C'_{NB}] two-dimensional fit in bins of the $m(K^+K^-)$ and $m(K^+\pi^0)$ distributions after applying the orthogonal requirements $m(K^+\pi^0) > 1.5$ GeV/c^2 and $m(K^+K^-) > 2.0$ GeV/c^2, respectively. These requirements suppress kinematic reflections. Figure 3 shows the resulting signal yields along with their statistical errors. With these data, we cannot make any definitive statement about possible intermediate K^+K^- resonances, including the structure seen by *BABAR* near 1.5 GeV/c^2 [6]. It is worth noting here that the recent LHCb study of $B^\pm \to K^+K^-\pi^\pm$ decays [7] has revealed an unidentified structure in the same mass range; however, it is only present in B^+ events, giving rise to a large local *CP* asymmetry. Furthermore, we observe some excess of events around 1.4 GeV/c^2 in the $K^+\pi^0$ invariant-mass spectrum. A detailed interpretation will require an amplitude analysis with higher statistics that would be available at a next-generation flavor factory [26].

In summary, we report measurement of the suppressed decay $B^0 \to K^+K^-\pi^0$ using the full $\Upsilon(4S)$ data sample collected with the Belle detector. We employ a two-dimensional fit for extracting the signal yield. Our measured

branching fraction $\mathcal{B}(B^0 \to K^+K^-\pi^0) = [2.17 \pm 0.60(\text{stat}) \pm 0.24(\text{syst})] \times 10^{-6}$ constitutes the first evidence for the decay.

[1] B. Aubert *et al.* (*BABAR* Collaboration), Phys. Rev. D **75**, 012008 (2007).

[2] T. Aaltonen *et al.* (CDF Collaboration), Phys. Rev. Lett. **108**, 211803 (2012).

[3] R. Aaij *et al.* (LHCb Collaboration), J. High Energy Phys. 10 (2012) 037.

[4] Y. T. Duh *et al.* (Belle Collaboration), Phys. Rev. D **87**, 031103 (2013).

[5] B. Aubert *et al.* (*BABAR* Collaboration), Phys. Rev. Lett. **97**, 171805 (2006).

[6] B. Aubert *et al.* (*BABAR* Collaboration), Phys. Rev. Lett. **99**, 221801 (2007).

[7] R. Aaij *et al.* (LHCb Collaboration), Report No. LHCb-CONF-2012-028, 2012.

[8] Throughout this paper, inclusion of the charge-conjugate process is implied unless otherwise explicitly mentioned.

[9] E. Eckhart *et al.* (CLEO Collaboration), Phys. Rev. Lett. **89**, 251801 (2002).

[10] J. H. Kim *et al.* (Belle Collaboration), Phys. Rev. D **86**, 031101 (2012).

[11] S. Bar-Shalom, G. Eilam, and Y. D. Yang, Phys. Rev. D **67**, 014007 (2003).

[12] D. S. Du, H. J. Gong, J. F. Sun, D. S. Yang, and G. H. Zhu, Phys. Rev. D **65**, 094025 (2002); **66**, 079904(E) (2002).

[13] M. Beneke and M. Neubert, Nucl. Phys. **B675**, 333 (2003).

[14] L. Guo, Q. G. Xu, and Z. J. Xiao, Phys. Rev. D **75**, 014019 (2007).

[15] A. Garmash *et al.* (Belle Collaboration), Phys. Rev. D **71**, 092003 (2005).

[16] Y. Nakahama *et al.* (Belle Collaboration), Phys. Rev. D **82**, 073011 (2010).

[17] J. P. Lees *et al.* (*BABAR* Collaboration), Phys. Rev. D **85**, 112010 (2012).

[18] A. Abashian *et al.* (Belle Collaboration), Nucl. Instrum. Methods Phys. Res., Sect. A **479**, 117 (2002); also, see the detector section in J. Brodzicka *et al.*, Prog. Theor. Exp. Phys., 04D001 (2012).

[19] S. Kurokawa and E. Kikutani, Nucl. Instrum. Methods Phys. Res., Sect. A **499**, 1 (2003), and other papers included in this volume; T. Abe *et al.*, Prog. Theor. Exp. Phys., 03A001 (2013) and following articles up to 03A011.

[20] J. Beringer *et al.* (Particle Data Group), Phys. Rev. D **86**, 010001 (2012).

[21] M. Feindt and U. Kerzel, Nucl. Instrum. Methods Phys. Res., Sect. A **559**, 190 (2006).

[22] S. H. Lee *et al.* (Belle Collaboration), Phys. Rev. Lett. **91**, 261801 (2003).

[23] D. J. Lange, Nucl. Instrum. Methods Phys. Res., Sect. A **462**, 152 (2001).

[24] T. Skwarnicki, DESY Report No. F31-86-02, 1986.

[25] J. P. Lees *et al.* (*BABAR* Collaboration), Phys. Rev. D **83**, 112010 (2011).

[26] T. Abe *et al.* (Belle II Collaboration), arXiv:1011.0352.